Indian Journal of Pure & Applied Physics
Vol. 63, June 2025, pp. 451-459
DOI: 10.56042/ijpap.v63i6.8481

Hybrid Nanofluid Flow for Mixed Convection along a Vertical Sheet in Presence of Porous Media with Heat Source, Variable Temperature, and Thermal Radiation

Ram Prakash Sharma[1], Seema Tinker[2], Om Prakash[2*] & Brajesh Kumar Kulshrestha[3]

[1]Department of Mechanical Engineering, National Institute of Technology Arunachal Pradesh, Arunachal Pradesh 791 113, India

[2]Department of Mathematics, JECRC University, Jaipur 303 905, India

[3]Department of Mathematics, National Institute of Technology Arunachal Pradesh, Arunachal Pradesh 791 113, India

Received: 1 February 2024; accepted: 21 May 2025

The study of a hybrid nanofluid flowing in a mixed convection along a vertical sheet in the presence of porous media with heat source, variable temperature, and thermal radiation is examined. By the similarity transformation, the governing equations are transformed into non-dimensional differential equations and solved with the help of the shooting technique using the Runge-Kutta method. The physical significance of the contributive parameters through graphs and tables are presented by the bvp4c solver in Matlab software and found that an increase in the heat source, thermal radiation, and mixed convection increases the fluid velocity of the hybrid nanofluid. The inclusion of variable temperature boundary conditions leads to a decrease in fluid velocity and temperature with the involvement of the particle concentration.

Keywords: Heat source, Hybrid nanofluid, Thermal radiation, Mixed convection, Variable temperature boundary problem

1 Introduction

Researchers have been concerned with the improvement of heat transfer rates in diverse thermal systems. For example, in the engine of an automobile temperature increases between stationary and moving parts of the system. The performance of the engine depends on the heat removal property of a lubricant. Enhancement of thermal conductivity of lubricant increases the ability of cooling/heating. Since it is known that in comparison to fluids, solids have greater thermal conductivity. It gave thought to mixing solids with fluids to enhance effective conductivity.

Choi and Eastman first introduced the name nanofluid, prepared by synthesizing nanometer-sized (1-100nm) particles of metal or metal oxides, etc. with base fluids[1]. There are more advantages to the use of nanofluids as compared with only base fluids. Several applications in different fields like heat transfer, heat conservation, medicine, electronics, automobiles, etc. motivated researchers to more and more investigations in this field. Using Buongiorno's model, Rosca and Pop examined an unsteady boundary layer flow over a moving sheet in an external free stream[2]. Sheikholeslami and Sadoughi have studied the enrichment of heat transfer of nanofluid with the magnetic field[3]. In this paper, PDEs are solved using the macroscopic method CVFEM. Waqas *et al*. have evaluated the effect of viscous dissipation in nanofluid over a stretch cylinder by the bvp4c method and the study determined that an escalation in the nanofluid volume fraction results in a rise in the velocity[4]. Using the RKF method, Kumar *et al.* inspected the heat transfer of nanoliquid flow through a curved stretching sheet[5].

A hybrid nanofluid is a fluid that contains two or more distinct nanoparticles in the base fluid. Hybrid nanofluid has been widely used in many areas such as engine cooling, biomedical, lubrication, microelectronic, and for a better heat transfer mechanism. Rostami *et al.* analyzed the laminar MHD flow of a hybrid nanofluid by the RKF method with the bvp4c method in Matlab for obtaining the solution and they observed that in the hybrid nanofluid flow, dual results exist for both opposing and assisting regimes[6]. Saba *et al.* have studied the heat transfer phenomena for the hybrid nanoliquid using the shooting technique with the R-K Filberg method to compute the system of ODEs[7]. It is seen that hybrid nanofluid temperature distribution plays a major role, as compared to nanofluid. Ma *et al.* investigated the heat transfer in a channel when active coolers and heaters were used with a hybrid nanofluid by the

*Corresponding author: (E-mail: om.prakash1@jecrcu.edu.in)

Lattice Boltzmann method[8]. The study indicated that by adding hybrid nanofluid with water the heat transfer rate increases. Waini *et al.* analyzed the unsteady hybrid nanofluid flow past an enlarging surface and they described the effects of the unsteadiness parameter and solid volume fraction for velocity and temperature profiles[9].

The heat transfer mechanism involves a combination of natural and forced convection, which is called mixed convection. The mixed convection flow is frequently used in nuclear reactors, technology, and engineering equipment. Xia *et al.* analyzed the effect of hybrid nanofluid on MHD mixed convective flow with multiple slip conditions[10]. Othman *et al.* analyzed mixed convection motion past a stretching/shrinking surface in a nanofluid[11]. They indicated that a rise in the mixed convention increases the velocity distribution. Using the finite difference method (FDM), Cimpean *et al.* explored the impact of mixed convection on a hybrid nanofluid within a porous trapezoidal chamber[12]. The problem indicated that high values of the Reynolds number describe forced convection and low values of Reynolds number indicate the development of mixed convection. Khashi'ie *et al.* have examined the non-Darcy combined convention of a hybrid nanoliquid[13]. The researchers noted that in the case of a hybrid nanofluid, an escalation in the mixed convection parameter results in an escalation in momentum distribution and a decrease in energy distribution. Wahid *et al.* reported the mixed convection hybrid nanofluid flow over a perpendicular sheet with thermal radiation and they observed that due to the mixed convection parameter, the heat transfer rate and skin friction coefficient increased[14]. Khan *et al.* investigated the impact of radiative mixed convection flow of a hybrid nanofluid through a vertical cylinder[15].

A porous media contains holes or pores through which fluid flows and is useful in many aspects of applied science and biomedical like tissue replacement, air conditioning, phase change material, material science, solar system, drug delivery, and geophysics. Sajjadi *et al.* have inspected the impact of MHD natural convection in a porous medium with a hybrid nanofluid and reported that due to porosity, the heat transfer rate was reduced[16]. Alkanhal *et al.* studied the MHD nanofluid flow in the presence of thermal radiation, heat source, and magnetic force inside a porous medium by the control volume finite element (CVFE) method[17]. Mehryan *et al.* analyzed the natural convection hybrid nanofluid flow through porous media using the Galerkin finite element method[18]. Wahid *et al.* investigated the Marangoni hybrid nanofluid flow through a permeable disk in the presence of porous media and observed that if porous medium intensity increased, the local Nusselt number also increased[19]. Daoud *et al.* have explored the 3D MHD flow past a stretching surface in the presence of a porous medium, and they showed that the reduction of the permeability parameter decreases the velocity distribution[20].

Grubka and Bobba explored heat transport over a continuous linearly stretching surface using the power law temperature distribution[21]. Risbeck *et al.* have studied the laminar mixed convection flow through the horizontal sheet with variable temperatures using the FDM[22]. Cheng studied the transfer phenomenon of heat and mass for natural convection through a vertical plate with variable temperature and permeable medium in the presence of a transverse magnetic field[23]. Cao *et al.* analyzed the slip effect on the mixed convective boundary layer motion and heat transport over a perpendicular sheet[24]. Subhashini *et al.* have examined the mixed convective nanofluid flow through a moving vertical plate[25]. Reddy *et al.* have studied the heat transfer of a viscoelastic polymeric fluid on the semi-infinite vertical plate using Crank-Nicolson FDM for numerical solutions[26]. Mahmoudi examined the fluid metal free convection between perpendicular plates under a crosswise magnetic field[27]. Rajesh *et al.* have investigated the MHD hybrid nanoliquid motion over a vertical sheet with a raged temperature of the wall[28].

Wahid *et al.* illustrated the MHD flow of a hybrid nanofluid over a vertical plate in the presence of thermal radiation and they reported that fluid temperature increased due to an escalation in the radiation parameter[29]. Waqas *et al.* considered the thermal radiation impact on nanofluid past a porous cylinder[30]. Abbasi *et al.* explored the impact of nonlinear thermal radiation on a hybrid nanofluid and they found that the temperature of the fluid increases with an increase in the radiation parameter[31]. Khan *et al.* inspected the effect of thermal radiation on the mixed convective motion of a hybrid nanofluid and they found that the fluid temperature was enriched due to radiation[32]. Sivasankaran *et al.* deliberated the thermal radiation effect on a hybrid nanofluid flow between parallel sheets and found a decrease in temperature due

to an increment in thermal radiation[33]. Ullah *et al.* examined the significance of heat source on magnetized nanofluid through the radial disk and the result showed that the heat source parameter enhanced the temperature profile[34].

Tayebi *et al.* studied the impact of heat source/sink on a hybrid nanofluid in a circular annulus[35]. Jamaludin *et al.* examined the impact of MHD mixed convective motion of hybrid nanofluid through an enlarging surface with a heat sink/source and they found accelerated separation of the boundary layer due to heat source[36]. Azam *et al.* determined the effect of heat source/sink in unsteady cross nanofluid over a shrinking/stretching cylinder and they reported that the mass transfer rate and boundary layer thickness increased due to heat source[37]. Mansour *et al.* explored the influence of heat source/sink, heat transfer, and MHD on the natural convection flow of hybrid nanofluids using the FDM method[38]. They observed that the sustainability of hybrid nanofluid decreased due to heat source. Ratha *et al.* investigated the unsteady 2D flow of an incompressible Casson nanofluid over a shrinking horizontal sheet with an inclined magnetic field and Joule heating[39]. Using the Buongiorno model, they found that the Casson parameter and suction/injection enhance velocity profiles, while Brownian motion and thermophoresis augment fluid temperature. Baag *et al.* numerically investigated the magnetohydrodynamic flow of a viscous liquid past an expanding sheet embedded in a permeable medium, considering thermal buoyancy, heat source/sink, chemical reaction, convective heating, and cross-diffusion effects[40]. Using Runge-Kutta fourth-order with shooting in MATLAB's bvp5c, they found that thermal buoyancy enhances velocity, while convective heating augments fluid temperature.

Tinker *et al.* numerically analyzed the heat transfer of a time-dependent hybrid nanofluid flow with thermal radiation and heat source/sink over a stretching/shrinking sheet[41]. Using similarity transformations and MATLAB's bvp5c, they found dual solutions depending on the unsteadiness parameter. Stability analysis revealed one stable and one unstable solution. The study also showed that second-order slip significantly impacts flow and heat transfer, and increasing suction enhances frictional stress and heat transfer. Pattnaik *et al.* studied the free convection of an electrically conducting viscoelastic nanofluid over an expanding surface, considering Brownian motion, thermophoresis, thermal radiation, and chemical reaction[42]. They used a hybrid perturbation method and the MATLAB bvp4c solver to analyze the transformed ordinary differential equations. Their findings highlighted the influence of various physical parameters on the flow and heat transport, with implications for industrial processes. Panda *et al.* numerically investigated heat transport in buoyant wedge-shaped flow of SWCNT-MWCNT hybrid nanofluid over a radiative vertical permeable wedge with variable wall temperature and heat source/sink[43]. Their key findings indicate that heat transport is enhanced by linear radiation, nanoparticle volume fraction, and uniform heat source, while momentum is influenced by wedge angle and nanoparticle volume fraction. Mixed convection parameters increase the momentum boundary layer.

Baag *et al.* numerically examined the magnetohydrodynamic flow of a viscous liquid over an expanding sheet in a permeable medium, considering thermal buoyancy, heat source/sink, chemical reaction, convective heating, and cross-diffusion[44] (Brownian motion and thermophoresis). Using Runge-Kutta fourth-order with shooting in MATLAB's bvp5c, they found that thermal buoyancy enhances velocity, and convective heating increases fluid temperature. Pattnaik *et al.* numerically investigated the buoyant flow of a conducting time-dependent nanofluid (gold nanoparticles in water, modeled by Hamilton-Crosser's model) through porous moving walls filled with a porous medium, considering a uniform heat source and absorption[45]. Using Runge-Kutta fourth-order method their findings indicate that nanoparticle volume concentration enhances fluid velocity in the channel's middle layer but retards it near the walls. Additionally, increasing Reynolds number and wall heating/cooling augment shear stress. The study suggests potential applications in biotechnology. Merkin has analyzed the impact of mixed convection motion through a perpendicular sheet in a saturated permeable medium[46]. Ahmed and Pop investigated the effect of mixed convection flow of nanofluid past a vertical plate with permeable medium[47]. Waini *et al.* studied the mixed convection motion of a hybrid nanoliquid over a vertical needle with surface heat flux[48].

The main aim of this study is to investigate a hybrid nanofluid flow in mixed convection along a perpendicular sheet in the existence of porous media with a heat source, variable temperature, and thermal radiation. The investigation incorporates the effects of

various factors on the momentum and temperature distributions such as thermal radiation, heat source, and variable temperature boundary conditions to study the steady mixed convective boundary layer flow along a perpendicular flat plate enclosed in a permeable medium.

2 Mathematical Formulation

This paper examines the mixed convection steady flow on an impermeable vertical surface immersed in a porous medium filled with a hybrid nanofluid, incorporating thermal radiation, heat source, and a variable temperature boundary problem. Figure 1 shows the $x-$axis measured along the plate and the $y-$axis perpendicular to it. The velocity components along the x and $y-$axis are denoted by u and v, respectively. The free stream velocity is represented as U_∞, while T_w and T_∞ are the constant surface temperature and the constant free stream temperature, respectively, with $T_w > T_\infty$ (heated plate) for assisting flow and $T_w < T_\infty$ (cooled plate) for opposing flow. Additionally, the study assumes that the nanoparticles have a uniform size, and agglomeration of nanoparticles is neglected since the hybrid nanofluid is synthesized as a stable compound.

The hybrid nanofluid equations are derived by utilizing the standard approximations of the boundary layer, as outlined in Merkin[46] and Ahmad and Pop[47].

$$\frac{\partial u}{\partial x}+\frac{\partial v}{\partial y}=0, \qquad \ldots (1)$$

$$u=U_\infty+\frac{gK(\rho\beta)_{hnf}}{\mu_{hnf}}\left(T-T_\infty\right), \qquad \ldots (2)$$

$$u\frac{\partial T}{\partial x}+v\frac{\partial T}{\partial y}=\frac{k_{hnf}}{(\rho c_p)_{hnf}}\frac{\partial^2 T}{\partial y^2}-\frac{1}{(\rho c_p)_{hnf}}\frac{\partial q_r}{\partial y}+\frac{Q_0}{(\rho c_p)_{hnf}}\left(T-T_\infty\right), \qquad \ldots (3)$$

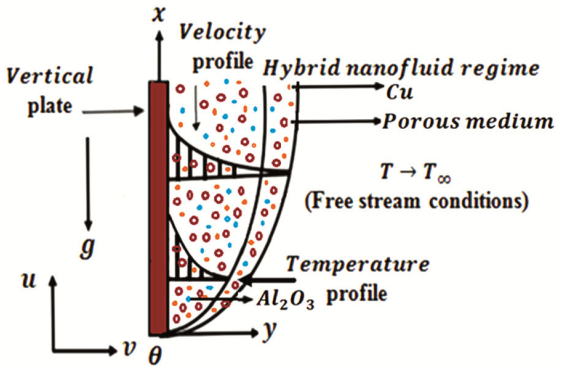

Fig. 1 — Flow behavior of a model

subjected to:

$$\left.\begin{aligned} v=0, \quad & T=T_\infty+Ax^\gamma \ \text{ at } y=0 \\ u\to U_\infty, \quad & T\to T_\infty \quad \text{as } y\to\infty \end{aligned}\right\} \qquad \ldots (4)$$

Here the temperature of a hybrid nanofluid is represented by T, porous medium permeability by K, variable temperature index by γ, and acceleration due to gravity by g. Further, dynamic viscosity is represented by μ_{hnf}, density by ρ_{hnf}, thermal conductivity by k_{hnf}, thermal expansion coefficient by β_{hnf}, and hybrid nanofluid heat capacity by $(\rho c_p)_{hnf}$.

The Rossel and approximation is employed for q_r

$$q_r=-\frac{4\sigma^*}{3k^*}\frac{\partial T^4}{\partial y}, \qquad \ldots (5)$$

The T^4 expressed in Taylor's series about T_∞ in which higher order terms are removed[48],

$T^4 \approx 4TT_\infty^3-3T_\infty^4$,

Then Eq (3) changed as follows

$$u\frac{\partial T}{\partial x}+v\frac{\partial T}{\partial y}=\frac{k_{hnf}}{(\rho c_p)_{hnf}}\frac{\partial^2 T}{\partial y^2}+\frac{1}{(\rho c_p)_{hnf}}\frac{16}{3}\frac{\sigma^*}{k^*}T_\infty^3\frac{\partial^2 T}{\partial y^2}+\frac{Q_0}{(\rho c_p)_{hnf}}\left(T-T_\infty\right), \qquad \ldots (6)$$

Now, the following variables are used to get the similarity solutions of Eqs (1), (2), and (6) are:

$$\psi=\left(2\alpha_f U_\infty x\right)^{1/2}f(\eta),\theta(\eta)=\frac{(T-T_\infty)}{(T_w-T_\infty)},\ \eta=\left(\frac{U_\infty}{2\alpha_f x}\right)^{1/2}y, \qquad \ldots (7)$$

here, ψ = stream function, $u=\frac{\partial\psi}{\partial y}$ and $v=-\frac{\partial\psi}{\partial x}$, α_f = fluid thermal diffusivity. The variable taken in (7) satisfies the Eq. of continuity (1), and we have:

$$f'=1+\frac{\mu_f}{\mu_{hnf}}\frac{(\rho\beta)_{hnf}}{(\rho\beta)_f}\lambda\theta, \qquad \ldots (8)$$

$$\left(\frac{\alpha_{hnf}}{\alpha_f}+\frac{(\rho c_p)_f}{(\rho c_p)_{hnf}}\frac{4}{3}Rd\right)\theta''+f\theta'-2\gamma f'\theta+Q\theta=0, \qquad \ldots (9)$$

Table 1 — Thermo-physical properties (Fluid and nanoparticles)

Fluids	$c_p(j/kgK)$	$\rho(kg/m^3)$	$k(W/mK)$	$\sigma(S/m)$	$\beta(1/K)$
H_2O	4179	997.1	0.613	0.05	21×10^{-5}
Al_2O_3	765	3970	40	3.69×10^{7}	0.85×10^{-5}
Cu	385	8933	400	5.96×10^{7}	1.67×10^{-5}

Subjected to:

$$\left.\begin{array}{lll} f(\eta)=0, & \theta(\eta)=1 & at\ \ \eta=0 \\ f'(\eta)\to 1, & \theta(\eta)\to 0 & \text{as}\ \ \eta\to\infty \end{array}\right\} \quad \ldots (10)$$

Here (') denotes diff. with respect to η and the parameter of mixed convection described by $\lambda=\frac{Ra_x}{Pe_x}$, with local Rayleigh number = $Ra_x=\frac{gK(\rho\beta)_f(T_w-T_\infty)x}{\mu_f\alpha_f}$ and local Péclet number $=Pe_x=\frac{U_\infty x}{\alpha_f}$. Here, $\lambda<0$ defines the opposing flow, $\lambda>0$ defines the assisting flow, and $\lambda=0$ defines the forced convection flow, respectively, here $Rd=\frac{4\sigma^* {T_\infty}^3}{k^* k_f}$ and $Q=\frac{2Q_0}{(\rho c_p)_{hnf}}\frac{x}{U_\infty}$ are thermal radiation parameter and heat source parameters, respectively.

The skin friction coefficient and Nusselt number in terms of shear stress τ_w and heat flux q_w given as

$$C_f=\frac{\tau_w}{\rho_f U_\infty^2}, \quad \ldots (11)$$

$$Nu_x=\frac{xq_w}{k_f(T_w-T_\infty)}, \quad \ldots (12)$$

$$\tau_w=\mu_{hnf}\left(\frac{\partial u}{\partial y}\right)_{y=0}, \quad \ldots (13)$$

$$q_w=-k_{hnf}\left(\frac{\partial T}{\partial y}\right)_{y=0} \quad \ldots (14)$$

Using (5), (11), (12), (13), and (14), we get:

$$\left(\frac{2\,\mathrm{Re}_x}{\mathrm{Pr}}\right)^{1/2} C_f=\frac{\mu_{hnf}}{\mu_f}f''(0), \quad \ldots (15)$$

$$\left(\frac{2}{\mathrm{Re}\,\mathrm{Pr}}\right)^{\frac{1}{2}} Nu_x=-\frac{k_{hnf}}{k_f}\theta'(0), \quad \ldots (16)$$

Where the Prandt l number $\mathrm{Pr}=\frac{\nu_f}{\alpha_f}$ and the local Reynolds number $\mathrm{Re}_x=\frac{U_\infty x}{\nu_f}$, ν_f is the fluid kinematic viscosity.

3 Results and Discussion

The bvp4c procedure in MATLAB systems software was used to solve the transformed non-linear ODEs (9) and (10) along with boundary conditions (11). This procedure converted the transformed boundary value problem into a system of 1st ODEs. The investigation focused on motion phenomena and various graphs were used to present the momentum and temperature distributions for distinct parameter values. The fixed parameters for which the results were presented are taken as $Q=0.1, Rd=1, \phi_1=0.1, \phi_2=0.04, \gamma=0.3, \lambda=1$ for velocity graphs and $Q=0.1, Rd=1, \phi_1=0.1, \phi_2=0.04, \gamma=0.1, \lambda=-1$ for temperature graphs, and they may vary whenever required. In Fig. 2, the impact of radiation on velocity is illustrated. The increment in radiation parameter intensifies the random movement of nanoparticles, which, in turn, results in frequent collisions and additional heat generation. As a result, an increase in temperature and velocity can be observed.

Figure 3 highlights the physical behavior of the velocity profile for various values of λ keeping other dimensionless parameters fixed. Mixed convection occurs when both natural (driven by buoyancy forces) and forced (driven by external forces) convection mechanisms are present. The behavior of fluid motion and transfer of heat is significantly influenced by the parameter of mixed convection. When the mixed convection parameter increases, it displays a corresponding rise in fluid velocity. This is because an increase in λ leads to an increase in the buoyancy force, which in turn affects the speed of the fluid flow as determined by the ratio of the temperature

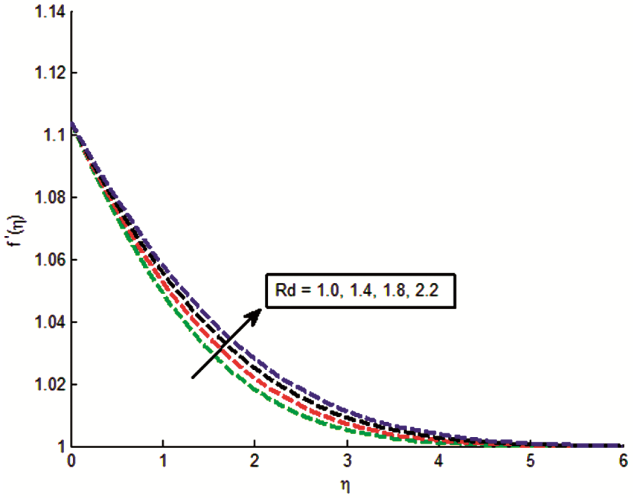

Fig. 2 — Velocity depiction for Rd

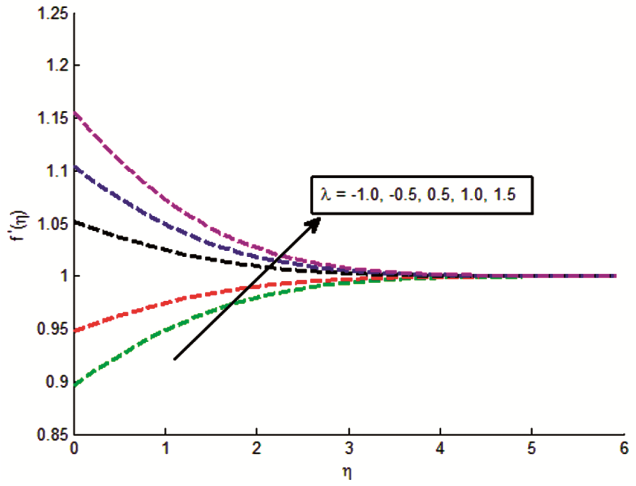

Fig. 3 — Velocity depiction for λ

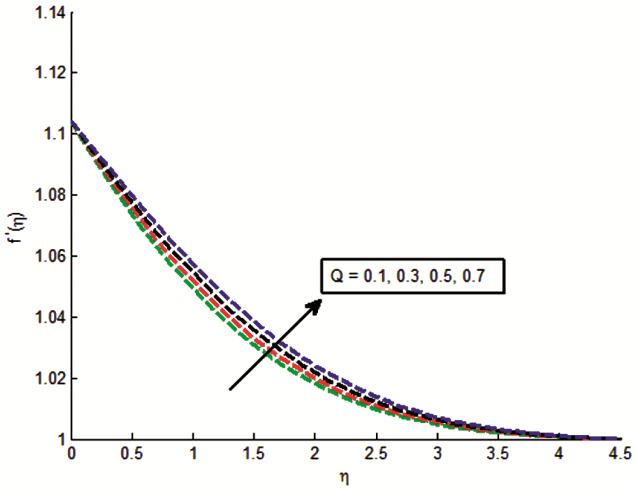

Fig. 4 — Velocity depiction for Q

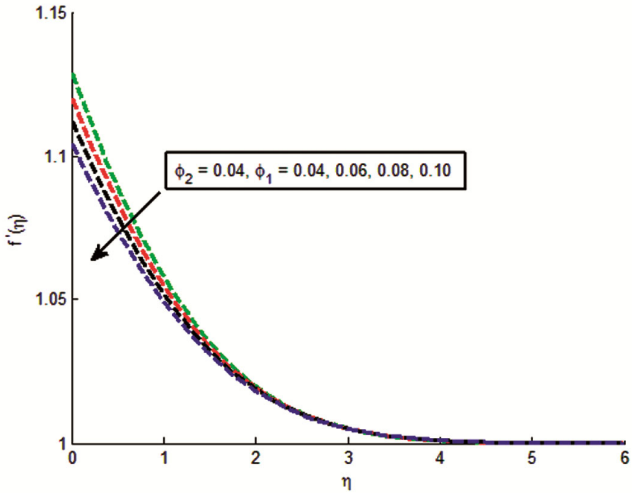

Fig. 5 — Velocity depiction for ϕ_1

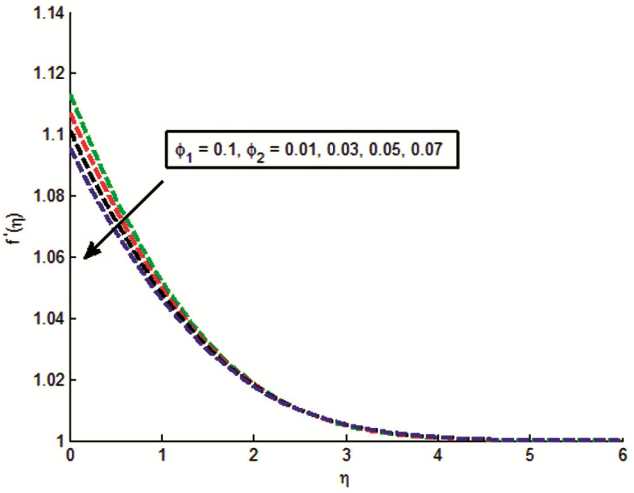

Fig. 6 — Velocity depiction for ϕ_2

difference and inertial force. The contribution of natural convection to fluid flow increases when the mixed convection parameter rises.

The positive correlation between fluid velocity and heat source/sink parameter is evident in Fig. 4. In the case of the heat source scenario, the thermal boundary layer's thickness rises due to a rise in the heat source parameter. This, in turn, leads to a rise in internal heat energy, increasing fluid velocity. Figures 5 and 6 show the momentum distribution of $Al_2O_3 / Cu - water$ based hybrid nanofluid. According to the findings of Fig. 5, a rise in the volume fraction of Al_2O_3 nanoparticles causes clogging, which in turn causes a decrease in momentum. This effect is further supported by the velocity distribution, which shows that the width of the momentum boundary layer decreases as the volume fraction of Al_2O_3 increases. This same behavior has been shown in Fig. 6 that an increase in the volume fraction of (Cu) nano-particles causes a fall into momentum distribution. Figure 7 describes the impact of the variable temperature index γ on the velocity depiction. It is observed that an increment in γ leads to a decrement in the velocity profile.

Figure 8 exhibits the influence of heat source on fluid temperature. The profiles reveal that a rise in the heat source (Q) displays higher thermal conductivity, owing to the thickening of the thermal boundary layer. The phenomenon can be attributed to the larger contribution of heat from the dominant values of Q to the working fluid, which accelerates the thermal profile and, consequently, boosts the velocity and temperature of the fluid. By holding other

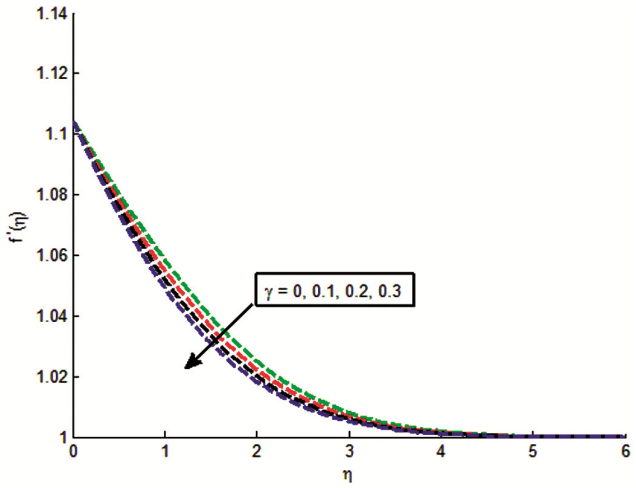

Fig. 7 — Velocity depiction for γ

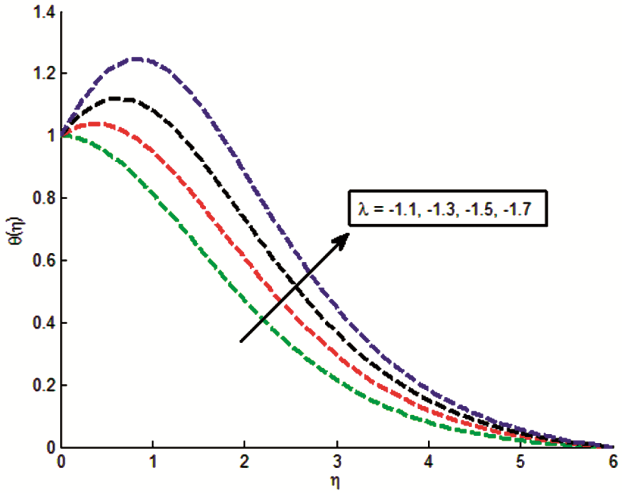

Fig. 9 — Temperature depiction for λ

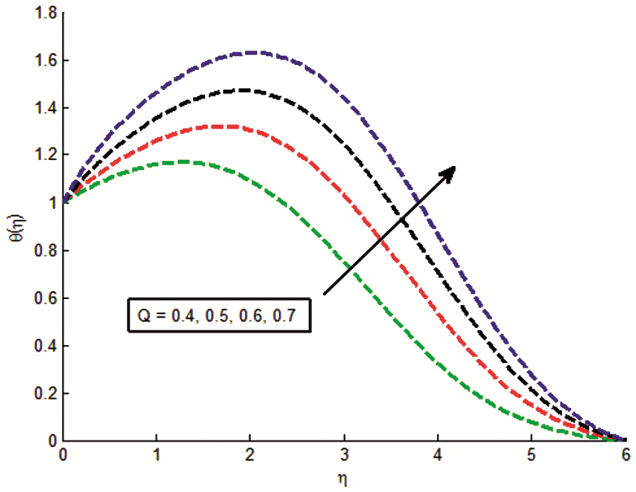

Fig. 8 — Temperature depiction for Q

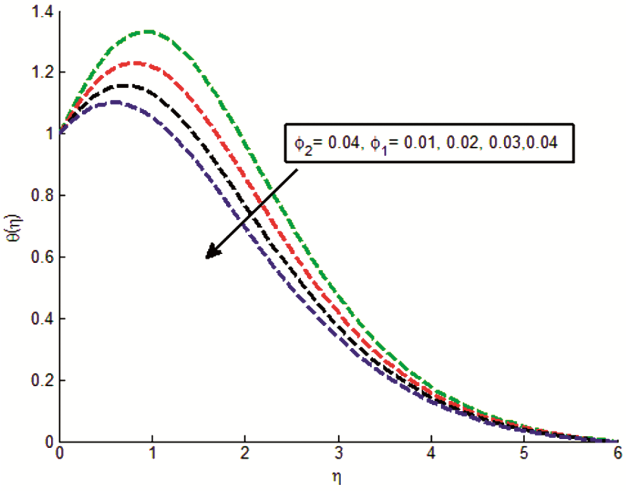

Fig.10 — Temperature depiction for ϕ_1

dimensionless parameters constant, Fig. 9 provides insight into the physical behavior of the temperature profile for various values of λ. The outcomes indicate that an increment in the mixed convection parameter (λ) provides a considerable rise in the observed temperature distribution due to a stronger influence of both forced convection (resulting from the external flow) and natural convection (due to buoyancy forces). Due to the opposing flow, the thermal boundary layer experiences an increase in thickness as the fluid velocity near the wall decreases, resulting in more internal heat energy being generated giving rise to the wall temperature.

Figures 10 and 11 illustrate the influence of volume fractions of $Al_2O_3 / Cu-water$ nanofluid on the temperature profile. The heat transfer performance is

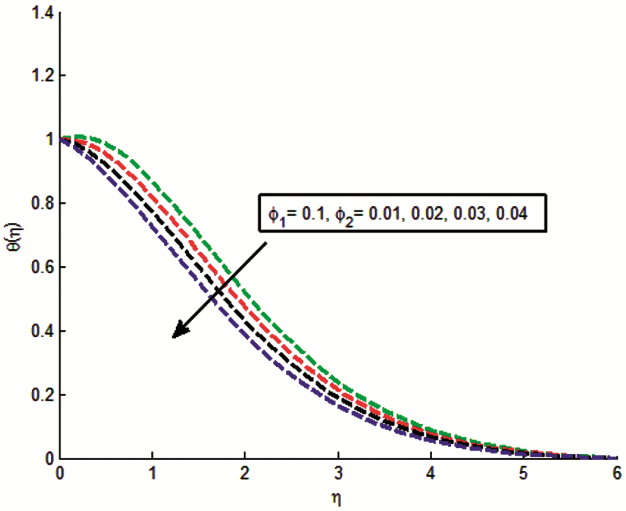

Fig.11 — Temperature depiction for ϕ_2

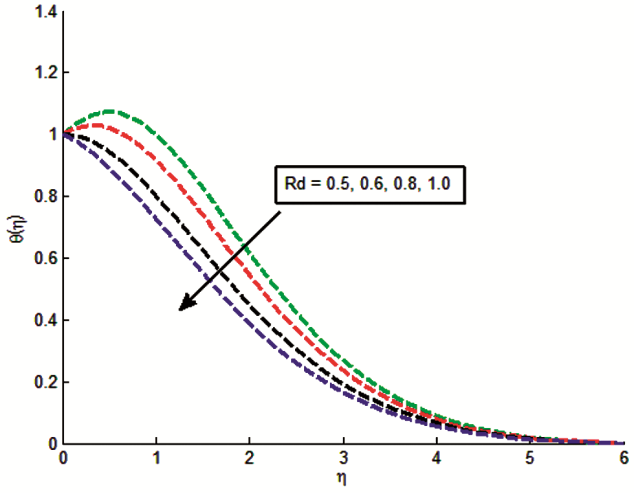

Fig.12 — Temperature depiction for *Rd*

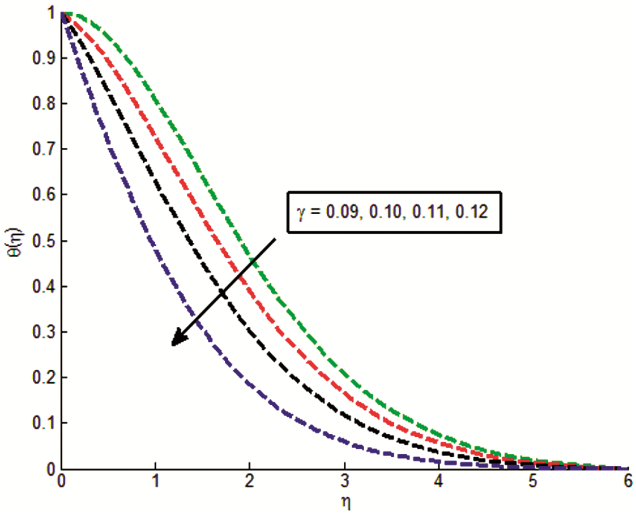

Fig. 13 — Temperature depiction for γ

observed to increase when the regular nanofluid is transformed into a hybrid nanofluid. This can be attributed to the enhanced mass of nanoparticles, leading to the development of convective heat transfer. Moreover, as the mass fractions of ϕ_1 (Al_2O_3) and ϕ_2 (Cu) increase, the surface temperature decreases, further augmenting this effect. Figure 12 depicts the influence of Rd on the temperature profile. As illustrated, an increase in Rd leads to a decrease in temperature, indicating an improvement in the heat transport rate. Hence, to facilitate the cooling process, it is recommended to minimize radiation. Figure 13 describes the impact of the variable temperature index γ on the temperature profile. It is observed that an increment in γ leads to a decrement in temperature profile.

4 Conclusion

The current research has expanded the scope of Merkin's seminal work [39] to include hybrid nanofluids. Our focus is on the flow of a steady mixed-convection boundary layer that occurs when a vertical semi-infinite flat plate is present in a porous media filled with hybrid nanofluid. The motion of the hybrid nanofluid was numerically examined using the bvp4c procedure in MATLAB systems software. The study examined the impacts of various working parameters, viz. nanoparticle volume fraction, heat source, mixed convection parameter, and thermal radiation parameter with variable temperature boundary problem. The key findings of the study can be précised as follows:

- The velocity profile rises with increasing values of heat source, mixed convection, and thermal radiation parameters and declines for higher values of Al_2O_3 and Cu nanoparticle volume fractions, and variable temperature index.
- A rise in heat source and mixed convection parameter values results in a rise in the temperature distribution.
- The temperature profile decreases with increasing values of nanoparticle volume fraction of Al_2O_3 and Cu nanoparticles, thermal radiation parameter, and variable temperature index.

References

1 Choi S U S & Eastman J A, *ASME International Mechanical Engineering Congress & Exposition*, 66 (1995) 99.
2 Rosca N C & Pop I, *Comp Fluids*, 95 (2014) 49.
3 Sheikholeslami M & Sadoughi M K, *Int J Heat Mass Transf*, 116 (2018) 909.
4 Waqas H, Yasmin S, Muhammad T & Imran M, *J Mater Res Technol*, 14 (2021) 2579.
5 Kumar R N, Gowda R J P, Alam M M, Ahmad I, Mahrous Y M, Gorji M R & Prasannakumara B C, *Int Comm Heat Mass Transf*, 126 (2021) 105445.
6 Rostami M N, Dinarvand S & Pop I, *Chin J Phys*, 56 (2018) 2465.
7 Saba F, Ahmed N, Khan U & Mohyud-Din S T, *Int J Heat Mass Transf*, 136 (2019) 186.
8 Ma Y, Mohebbi R, Rashidi M M & Yang Z, *Int J Heat Mass Transf*, 137 (2019) 714.
9 Waini I, Ishak A & Pop I, *Int J Heat Mass Transf*, 136 (2019) 288.
10 Xia W F, Ahmad S, Khan M N, Ahmad H, Rehman A, Baili J & Gia T N, *Case Studies Thermal Engg*, 32 (2022) 101893.
11 Othman N A, Yacob N A, Bachok N, Ishak A & pop I, *Applied Thermal Engg*, 117 (2017) 1412.
12 Cimpean D S, Sheremet M A & Pop I, *Int Comm Heat Mass Transf*, 116 (2020) 104627.

13 Khashi'ie N S, Arifin N M & Pop I, *Int Comm Heat Mass Transf*, 118 (2020) 104866.
14 Wahid N S, Md Arifin N, Khashi'ie N S, Pop I, Bachok N & Hafidzuddin E H, *Alex Engg J*, 61 (2021) 3323.
15 Khan U, Zaib A, Ishak A, Sherif E M, Waini I, Chu Y M & Pop I, *Case Studies Thermal Engg*, 30 (2022) 101711.
16 Sajjadi H, Delouei A A, Izadi M & Mohebbi R, *Int J Heat Mass Transf*, 132 (2019) 1087.
17 Alkanhal T A, Sheikholeslami M, Usman M, Haq R, Shafee A, Ahmadi A S & Tlili I, *Int J Heat Mass Transf*, 139 (2019) 87.
18 Mehryan S A M, Ghalambaz M, Chamkha A J & Izadi M, *Powder Technol*, 367 (2020) 443.
19 Wahid N S, Md Arifin N, Khashi'ie N S & Pop I, *Int Comm Heat Mass Transf*, 126 (2021) 105421.
20 Daoud Y, Abdalbagi M & Khidir A A, *Chin J of Phys*, 73 (2021) 232.
21 Grubka L J & Bobba K M, *ASME*, 107 (1985) 248.
22 Risbeck W R, Chen T S & Armaly B F, *Int J Heat Mass Transf*, 36 (1993) 1859.
23 Cheng C Y, *Int Comm Heat Mass Transf*, 32 (2005) 204.
24 Cao K & Baker J, *Int J Heat Mass Transf*, 52 (2009) 3829.
25 Subhashini S V & Sumathi R, *Int J Heat Mass Transf*, 71 (2014) 117.
26 Reddy G J, Kumar M & Beg O A, *Physica A Stat Mech Appl*, 510 (2018) 426.
27 Mahmoudi A, *Int Comm Heat Mass Transf*, 114 (2020) 104585.
28 Rajesh V, Sheremet M A & Oztop H F, *Case Stud Therm Engg*, 28 (2021) 101557.
29 Wahid N S, Md Arifin N, Khashi'ie N S, Pop I, Bachok N & Md Hafidzuddin E H, *Alex Engg J*, (2022) 61, 3323.
30 Waqas H, Yasmin S, Muhammad T & Imran M, *J Mater Res Technol*, 14 (2021) 2579.
31 Abbasi A, Gulzar S, Mabood F & Farooq W, *Int Commun Heat Mass Transf*, 126 (2021) 105335.
32 Khan U, Shafiq A, Zaib A & Baleanu D, *Case Stud Therm Engg*, 21 (2020) 100660.
33 Sivasankaran S, Bhuvaneswari M, Chandrapushpam T & Karthikeyan S, *Mater Today: Proc*, 82 (2021) 457.
34 Ullah I, Ullah R, Alqarni M S, Xia W & Muhammad T, *Int Commun Heat Mass Transf*, 126 (2021) 105416.
35 Tayebi T, Chamkha A J, Melaibari A A & Raouache E, *Int Commun Heat Mass Transf*, 126 (2021) 105397.
36 Jamaludin A, Naganthran K, Nazar R & Pop I, *Eur J Mech/B Fluids*, 84 (2020) 71.
37 Azam M, Xu T& Khan M, *Int Commun Heat Mass Transf*, 118 (2020) 104832.
38 Mansour M A, Siddiqa S, Gorla R S R & Rashad A M, *Therm Sci Engg*, 6 (2018) 57.
39 Ratha P K, Mishra S, Tripathy R & Pattnaik P K, *Proc Inst Mech Engg*, Part N. 237 (3-4) (2022) 83.
40 Baag S, Panda S, Pattnaik P K & Mishra S R, *J Nanomater, Nanoengg Nanosystem*, 236 (1-2) (2022) 19.
41 Pattnaik P K, Mishra S R, Panda S, Syed S A & Muduli K, *Math Probl Engg*, 2022 (2022) 2227811.
42 Panda S, Ontela S, Thumma T, Mishra S R & Pattnaik P K, *Mod Phys Lett B*, 38(1) (2024) 2350211.
43 Baag S, Panda S, Pattnaik P & Mishra S R, *Int J Ambient Energy*, 44 (1) (2023) 880.
44 Pattnaik P K, Abbas M A, Mishra S R, Khan S U & Bhatti M M, *CCHTS*, 25 (7) (2022) 1103.
45 Merkin J H, *J Engg Math*, 14 (1980) 4.
46 Ahmad S & Pop I, *Int Comm Heat Mass Transf*, 37 (2010) 987.
47 Waini I, Ishak A, Grosan T & Pop I, *Int Comm Heat Mass Transf*, 114 (2020) 104565.